HHS Public Access

Author manuscript

Cell Rep. Author manuscript; available in PMC 2015 November 21.

Published in final edited form as:

Cell Rep. 2015 November 17; 13(7): 1287–1294. doi:10.1016/j.celrep.2015.10.003.

The Stereociliary Paracrystal is a Dynamic Cytoskeletal Scaffold *In Vivo*

Philsang Hwang[1,2,◐], **Shih-Wei Chou**[1,2,◐], **Zongwei Chen**[1,2], and **Brian M. McDermott Jr.**[1,2,3,4,*]

[1]Department of Otolaryngology–Head and Neck Surgery, Case Western Reserve University School of Medicine, Cleveland, Ohio, 44106, United States of America

[2]Department of Biology, Case Western Reserve University, Cleveland, Ohio, 44106, United States of America

[3]Department of Genetics and Genome Sciences, Case Western Reserve University School of Medicine, Cleveland, Ohio, 44106, United States of America

[4]Department of Neurosciences, Case Western Reserve University School of Medicine, Cleveland, Ohio, 44106, United States of America

Summary

Permanency of mechanosensory stereocilia may be the consequence of either low protein turnover or protein renewal. Here we devise a system, using optical techniques in live zebrafish, to distinguish between these mechanisms. We demonstrate that the stereocilium's abundant actin cross-linker, fascin 2b, exchanges, without bias or a phosphointermediate, orders of magnitude faster ($t_{1/2}$ of 76.3 s) than any other known hair bundle protein. To establish the logic of fascin 2b's exchange, we examine whether filamentous actin is dynamic and detect substantial β-actin exchange within the stereocilium's paracrystal ($t_{1/2}$ of 4.08 h). We propose fascin 2b's behavior may enable cross-linking at fast timescales of stereocilia vibration while also noninstructively facilitating the slower process of actin exchange. Furthermore, tip protein myosin XVa fully exchanges in hours ($t_{1/2}$ of 11.6 h), indicating that delivery of myosin-associated cargo occurs in mature stereocilia. These findings suggest that stereocilia permanency is underpinned by vibrant protein exchange.

Graphical abstract

*Correspondence: bmm30@case.edu.
◐These authors contributed equally to this work.

Supplemental Information

Supplemental Information includes four figures, three tables, and one movie that can be found with this article online.

Author Contributions

P.H., S-W.C., and B.M.M. conceived the project, designed the experiments, and analyzed the data. P.H. and Z.C. performed FRAP experiments. S-W.C. carried out transgenesis and confocal imaging. P.H., S-W.C., and B.M.M. prepared the manuscript.

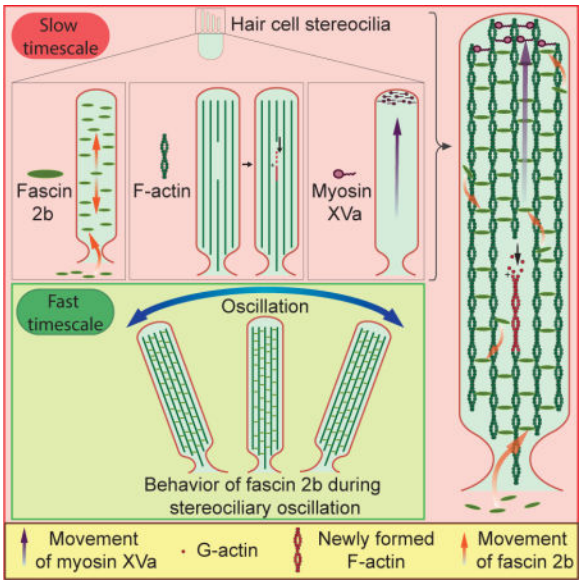

Introduction

In the ear, mechanotransduction for hearing and balance is initiated by stereocilia, which permanently crown each hair cell. Durability distinguishes stereocilia from other cellular protrusions, such as microvilli and filopodia, which are relatively short-lived (Edds, 1977; Gorelik et al., 2003). Stereocilia, extending from the hair cell's soma, are precisely arranged into a beveled hair bundle for transduction of mechanical stimuli (Manor and Kachar, 2008; Vollrath et al., 2007). A highly ordered parallel actin bundle, with a hexagonal cross-sectional configuration, forms a paracrystal essential to stereociliary function (Bartles, 2000; Schwander et al., 2010; Tilney et al., 1980). Actin-bundling and myosin motor proteins are necessary to organize stereociliary filamentous actin (F-actin) and contribute to the unique morphology and function of the hair bundle (Anderson et al., 2000; Boeda et al., 2002; Chou et al., 2011; Daudet and Lebart, 2002; Friedman et al., 2000; Gibson et al., 1995; Shin et al., 2010; Zheng et al., 2000). Although stereocilia are strikingly stable, the dynamics of the cytoskeletal proteins, which support these lever-like organelles through vigorous bouts of deflection that can exceed 100,000 Hz (Manley, 2012), are not clearly understood.

Studies on protein dynamics in stereocilia offer seemingly contrasting findings. Transfected, cultured, mammalian hair cells demonstrated that actin and actin-bundling protein espin are incorporated into the tip of each stereociliary paracrystal and treadmill ~5 μm per 24 h (Rzadzinska et al., 2004), indicating polymerization and cross-linking may be tightly coupled. In contrast, multi-isotope imaging mass spectrometry (MIMS), differential temporal expression of labeled actin proteins *in vivo*, and fluorescence recovery after photobleaching (FRAP) analyses in cultured cells demonstrated that in the shafts of stereocilia most protein (>90%) is stationary for up to a few weeks and actin does not treadmill (Zhang et al., 2012). In addition, stereociliary tips had higher rates of gross protein turnover and actin movement (Zhang et al., 2012). In agreement, a recent study using the technique of biolistic gene gun transfection of cDNAs into cultured utricular hair cells

demonstrated that exchange of F-actin seems to be restricted to the distal tip compartment of the mammalian stereocilium and accretion of actin at the tip is reliant on actin polymerization (Drummond et al., 2015).

In the present study, we develop a system that takes advantage of the optical transparency of zebrafish larvae to track the behavior of genetically-encoded, fluorescent, cytoskeletal proteins in the intact ear in real time. By peering directly into the whole ear, we reveal that the stereociliary paracrystal is a dynamic cytoskeletal scaffold, yielding insights into potential mechanisms of stereocilia function and longevity.

Results and Discussion

Fascin 2b exchange in the stereocilium is rapid and without bias or a phosphointermediate

To explore the fundamental behaviors of key proteins of the stereociliary paracrystal *in vivo*, we started by examining fascin 2b in larval zebrafish, exploiting the animal's optical transparency. Fascin 2 orthologous proteins contribute to stereociliary length (Chou et al., 2011; Perrin et al., 2013; Shin et al., 2010), and phosphorylation of serine 38 abolishes these proteins' capacities to bind and bundle F-actin (Chou et al., 2011; Lin-Jones and Burnside, 2007). To determine whether exchange of fascin 2b occurs in stereocilia or if it demonstrates immobility, as could be forecast by MIMS studies (Zhang et al., 2012), we tracked potential movement of fascin 2b in the zebrafish ear in real time. A novel stable transgenic was generated to express green fluorescent protein (GFP)-fascin 2b in hair cells. The stereocilia of the zebrafish otocyst were effectively and evenly labeled, and the fusion protein was minimally present in somata, faithfully mimicking endogenous localization (Figure 1B, Table S1, and Movie S1).

Initially, we characterized hair bundle development in lateral cristae, which contain the most accessible hair cells for FRAP in the otocyst, to determine a time point when formation decreases and most hair bundles are mature. At 4 days post-fertilization (dpf), hair cells are rapidly forming. By 7 dpf, hair bundle formation tapers off (Table S2), and the animals can hear and balance (Kimmel et al., 1974), indicating that most cells are mature. GFP-fascin 2b-containing hair bundles were analyzed by FRAP at 7 dpf; with a mean halftime for fluorescence recovery, $t_{1/2}$, of (mean halftime for fluorescence recovery ± standard error of the mean (SEM)) 76.3 ± 8.6 s (n = 11), fascin 2b exchange in stereocilia is surprisingly fast when the middle section of the bundle is bleached (Figures 1A–1E, 1J, and S1A). Protein exchange is defined as a protein that has moved and is traded for a bound protein. We assayed by FRAP the total amount of fascin 2b exchange, also known as the mobile fraction (Snapp et al., 2003), that occurred over a period of 60 minutes and determined that 82.5 ± 2.3% of the signal recovered (n = 3; data not shown). GFP-fascin 2b exchange rates were similar for hair bundles of 4-dpf and 7-dpf fish, demonstrating the exchange rate is not dependent on the developmental state of the bundle (Figures 1J, S1C-S1E, and S1G). Moreover, the GFP-fascin 2b exchange rate in hair bundles of the anterior macula, an auditory organ of the larval zebrafish, was similar in magnitude to that of crista, 36.6 ± 6.2 s (n = 5; data not shown). Interestingly, exchange rates of fascin 2b in stereocilia and fascin 1 in filopodia (Aratyn et al., 2007) contrast sharply, with the latter being an order of

magnitude faster (Figure 1J), perhaps because the extraordinarily high number of strands of F-actin slows exchange in stereocilia (relative to filopodia (Svitkina et al., 2003)).

To empirically ascertain whether the concentration of fascin 2b impacts the rate of fascin 2b exchange with F-actin *in vivo*, within stereocilia, we developed and performed the following FRAP-titration experiment. Briefly, transient transgenic fish, which have different amounts of GFP-fascin 2b in different hair bundles, were generated and used in FRAP experiments. If fascin 2b *in vivo* behaves similarly to fascin 1 *in vitro* (Courson and Rock, 2010), we would expect that hair cells expressing lower levels of fascin 2b would have corresponding decreased rates of exchange in stereocilia, relative to hair cells with higher levels of fascin 2b. If however the rates of exchange were similar in stereocilia with higher or lower levels of fascin 2b, then the rate of fascin 2b exchange is not dependent on concentration *in vivo*. Mosaic zebrafish, containing different amounts of GFP-fascin 2b in each hair bundle, as determined by relative levels of fluorescence, were generated and their hair bundles subjected to FRAP (Figure S1B). The rates of exchange were not dependent on the amount of fascin 2b in the hair bundle (Figure S1B). These results indicate that the behavior of fascin 2b *in vivo* in stereocilia is similar to fascin 1 behavior in live cellular protrusions (Aratyn et al., 2007; Li et al., 2010; Vignjevic et al., 2006) but is very different from the behavior of fascin 1 *in vitro* (Courson and Rock, 2010), where fascin 1 is relatively static when bound to pure F-actin (Courson and Rock, 2010). These differences can be explained by the finding that actin-bundling proteins can influence each other, such that one actin-bundling protein type can cause the displacement of another type in an actin bundle (Courson and Rock, 2010). Because stereocilia have at least a hundred different types of proteins (Shin et al., 2013), it may be that one or more of these proteins influence the kinetics of fascin 2b *in vivo*. These findings indicate that fascin 2b behavior is distinct from the behavior of espin, which treadmills (Rzadzinska et al., 2004) and undergoes total renewal in ~4 d within mammalian vestibular hair bundles. Thus, fascin 2b mobility within stereocilia is ~1,000-fold faster than espin and occurs through a fundamentally different mechanism.

We next considered whether fascin 2b exchange rates are asymmetric, *i.e.* faster near tips, as could be predicted by MIMS studies (Zhang et al., 2012). Surprisingly, when sections of the tops or bases of bundles were bleached, exchange rates were similar, $t_{1/2}$ = 55.2 ± 8.2 s (n = 5) or 54.1 ± 14 s (n = 6), respectively (Figures 1J and S2A–S2D). To resolve whether fascin 2b exchange was unidirectional or bidirectional, fluorescence was extinguished in top halves or bottom halves of bundles: movement in either direction was observed, indicating unbiased exchange (Figures 1F, 1G, and S2E–S2H). These results demonstrate that this abundant cross-linker of stereocilia exchanges rapidly and without bias (Figure 1I), contrasting significantly with predictions based on MIMS (Zhang et al., 2012) or espin cross-linker studies (Rzadzinska et al., 2004).

Protein entry into a microtubule-based cilium is regulated at the base by a size-exclusion permeability barrier (Kee et al., 2012). We next examined whether the mature stereocilium is, similarly, a privileged compartment: Is fascin 2b in the cell soma able to exchange with fascin 2b in stereocilia? After bleaching fluorescence in whole bundles, recovery was in fact observed (Figure 1H). Thus, GFP-fascin 2b, with a mass of 84 kDa, efficiently enters

stereocilia from the cell soma (Figures 1H and 1I), indicating that mature stereocilia are not a closed system for proteins with this mass or lower.

To probe this intriguing fascin 2b exchange mechanism for a role of phosphorylation, we developed a two-step strategy. First, a series of novel stable transgenics (Table S1) was generated to express, in hair cells, either a non-phosphorylatable fascin 2b phosphomutant (GFP-S38A) (Chou et al., 2011), a fascin 2b phosphomimetic (GFP-S38E) (Chou et al., 2011), or GFP (McDermott et al., 2010). The hair bundle-to-soma fluorescence intensity ratios (I_{bundle}/I_{soma}) of 7-dpf zebrafish were 29.3 ± 2.9 (n = 38), 23.3 ± 2.4 (n = 33), 0.68 ± 0.05 (n = 35), and 0.06 ± 0.01 (n = 32) for wild-type fascin 2b, GFP-S38A, GFP-S38E, and GFP, respectively (Table S3), establishing that phosphorylation diminishes the steady-state level of hair bundle-localized fascin 2b, a finding consistent with our previous investigation (Chou et al., 2011). Second, we assessed whether fascin 2b phosphorylation impacts this protein's stereociliary exchange rate by FRAP. GFP-fascin 2b and GFP-S38A had similar recovery rates, $t_{1/2}$ = 76.3 ± 8.6 s (n = 11) and $t_{1/2}$ = 75.5 ± 7.8 s (n = 11), respectively (Figures 2A–2C, 2G, and S1F). The fraction of phosphomimetic GFP-S38E that localized to the hair bundle moved much more rapidly, $t_{1/2}$ = 4.39 ± 0.37 s (17-fold faster; n = 12) (Figures 2D–2G), than wild-type protein. Taken together, these findings indicate that phosphorylation of fascin 2b does not play a significant role in the fascin 2b exchange mechanism within stereocilia, as the rate of wild-type fascin 2b recovery is not significantly faster than GFP-S38A (Figure S3). These data support a mechanism in which non-phosphorylated fascin 2b localizes to stereocilia, and only this form of fascin 2b exchanges, without a detectable phosphointermediate (Figure 2H).

β-actin exchange within the stereocilium's paracrystal occurs on an hourly timescale

To understand the logic of fascin 2b's rapid exchange, we characterized F-actin, the substrate of fascin 2b, in zebrafish stereocilia. One purpose of fascin 2b exchange could be to facilitate globular actin exchange withF-actin, should actin exchange occur in stereocilia. To examine F-actin behavior, we used 7-dpf transgenics, which have β-actin-mCherry localized to stereocilia (Antonellis et al., 2014), for FRAP and monitored recovery for 30 h (Figure 3). In contrast to previous studies (Zhang et al., 2012), β-actin-mCherry-containing hair bundles recovered fluorescence rapidly after bleaching, on an hourly timescale (Figures 3E and 3F): the mean halftime for fluorescence recovery, $t_{1/2}$, was 4.08 ± 0.92 h (n = 10) (Figure 4D), and the mean percentage of total fluorescence recovery over a 30 h time period was ~31 ± 5% (n = 11). The observed recovery was not treadmilling *en masse*, where all of the F-actin treadmills uniformly (Rzadzinska et al., 2004). With the above finding and the observation of intermittent gaps within the F-actin strands of stereocilia (Belyantseva et al., 2009), we propose a model that explains the recovery as one in which the strands of the stereociliary F-actin core in the shafts are discontinuous—possibly transiently–with free barbed ends along the length of each stereocilium that exchange with free globular actin (G-actin) (Figure S4B). A second, but not mutually exclusive, model that would fit these data and other data (Drummond et al., 2015; Narayanan et al., 2015; Zhang et al., 2012) is that actin is being systematically assembled and disassembled at the tips of stereocilia (Figure S4C). Importantly, the second model cannot explain all of the recovery of β-actin-mCherry because the very tips of stereocilia do not contain 31% of the actin.

Stereocilia tip protein myosin XVa fully exchanges in hours

Because MIMS showed an increased level of protein turnover at the tips of stereocilia (Zhang et al., 2012), we examined another protein, myosin XVa, which localizes near the tips (Belyantseva et al., 2003; Belyantseva et al., 2005). It is unknown if myosin motors exchange at the tips of stereocilia once stereociliary maturation, audition, and equilibrium are fully realized. Myosin XVa has intriguing qualities distinct from other bundle proteins: it accumulates at the tips of stereocilia in direct proportion to stereociliary length and governs stereociliary height (Belyantseva et al., 2005) (Figure 4A). To test explicitly whether myosin XVa is static or dynamic at the tips of mature stereocilia, we generated transgenic fish expressing GFP-myosin XVa in hair cells, which mirrored localization observed in mammals. The top halves of bundles that contain β-actin-mCherry (as a counterlabel) and GFP-myosin XVa were photobleached (Figure 4B). Fluorescent GFP-myosin XVa repopulated the tips of stereocilia on an hourly timescale ($t_{1/2}$ = 11.6 ± 3.6 h, n = 4; Figure 4C), amassing near the tips of the stereocilia to maintain the direct proportion of stereocilia length-to-myosin concentration. Thus, myosins are active in mature stereocilia, suggesting that delivery of associated cargo occurs in stereocilia even after maturity is achieved (Jia et al., 2009; Zhao et al., 1996). Notably, the rate of GFP-myosin XVa recovery in stereocilia is an order of magnitude slower than in filopodia (Belyantseva et al., 2005) (~10 min for full recovery; Figure 4D); though, the distance covered for recovery is similar between the two protrusions, suggesting that myosin movement rates are regulated by distinct mechanisms in different actin-based protrusions.

Fascin 2b exchange may enable cross-linking at fast timescales of stereocilia vibration while also noninstructively facilitating the slower process of actin exchange

We propose that the fascin 2b exchange rate ($t_{1/2}$ of 76.3 ± 8.6 s) may represent a golden mean, balancing two opposing functions: stable cross-linking at fast timescales and fluctuating local cross-linking at slower timescales. On the one hand, during deflections of stereocilia, fascin 2b proteins should serve as stationary cross-links relative to vibration rates. This is because the fascin 2b exchange rate is much slower than the rate of stereocilia deflections (sub-second timescale) and the intrastereociliary concentration of fascin 2b is extremely high (Shin et al., 2013) (Figure S4A). On the other hand, fascin 2b mobility may enable actin exchange in mature and functional hair cells of young fish and perhaps other vertebrates. This process may help maintain the actin cores of stereocilia throughout the life of the cell and may assist in repairing damaged cores after acoustic overexposure. Here, we show that globular actin exchanges with F-actin in stereocilia on an hourly timescale. In this proposed process, fascin 2b cross-linkers may dissociate to permit local F-actin disassembly and then re-cross-link during re-polymerization to enable reformation of the paracrystal (Figure S4B and S4C). Based on our FRAP data and biochemical data, which demonstrate that fascin 2b can bundle actin into parallel bundles similar to those found in stereocilia (Lin-Jones and Burnside B., 2009 and Chou et al., 2011), we propose possible models (Figure S4) in which most of the fascin 2b actively participates in bundling stereociliary actin. The ratio of the amount of fascin 2b that bundles stereociliary actin versus the amount of fascin 2b that is simply bound to stereociliary actin at any point in time remains to be determined. In addition, since fascin 2b exchanges without bias, this suggests that fascin 2b

plays a non-instructive role in the F-actin disassembly-re-polymerization process. Importantly, how fascin 2b may collaborate with other actin-bundling proteins, such as plastin (Daudet and Lebart, 2002) or espin (Zheng et al., 2000), to maintain the stereociliary paracrystal warrants study.

Why do measurements of protein dynamics in stereocilia vary with different technologies?

We observed *in vivo* in real time that individual stereociliary proteins (β-actin, fascin 2b, and myosin XVa) each exchange orders of magnitude faster than what has been observed previously in gross protein turnover studies (Zhang et al., 2012). One explanation for the differences between these studies is that Zhang *et al.* noted that ~94% of protein was stable in the shafts, and turnover is higher at tips over long periods (Zhang et al., 2012); therefore, it is plausible that the 6% that does exchange in the shafts consists of fascin 2b and/or β-actin, Figures S4B and S4C, evident in Figures 1–3, and the exchange at the tips is constituted partially by myosin XVa, Figure 4. A possible second reason for the differences is that zebrafish hair bundles have fundamentally different protein dynamics than those of frogs and mammals (Zhang et al., 2012). Together our findings indicate that the dynamics of specific cytoskeletal proteins within the hair bundle result primarily from protein exchange and mobilization rather than protein synthesis and degradation.

Experimental procedures

Fish

Wild-type Tübingen (Tü), Ppv3b-4, and *Tg(Parval3b:β-actin-mCherry)* zebrafish strains were used for this study.

Molecular biology

To construct a vector for expression of GFP-myosin XVa in zebrafish hair cells, mouse myosin XVa cDNA was amplified from pEGFP-C2-myo15a with primer pair Myo15a inf F (5′-GGACTCAGATCTCGAGATTCATGCACTCCATACGCAACCT-3′) and Myo15a inf R (5′-TAAGGATCCACCCGGGCGTCGACTCACAAGAGGGTGATCT-3′). The amplicon was subcloned into *Xho* I and *Xma* I digested pMT/PV3b/GFP/WT-fascin2b vector (In-Fusion HD cloning kit; Clontech) to generate pMT/PV3b/EGFP/Mmu myosin15a.

Transgenesis

Each transgenic strain was generated by co-injection of the desired cDNA construct (Table S1) and Tol2 RNA into one-cell stage zebrafish embryos (Balciunas et al., 2006).

FRAP acquisition and analysis

Embryonic or larval stage zebrafish were anesthetized in 650 μM 3-aminobenzoic acid ethyl ester methanesulfonate (Sigma–Aldrich) in fish water and then immobilized on glass-bottom dishes (MatTek) in 0.1% (wt/vol) low-melting-point agarose (Promega). The immobilized embryos were then covered with fish water containing 3-aminobenzoic acid ethyl ester methanesulfonate to prevent desiccation and twitching during time-lapse imaging.

FRAP experiments were conducted using laser scanning confocal microscopes (TCS SP2, SP5, or SP8; Leica Microsystems Inc.) with 40 × or 63 ×/1.4 NA oil-immersion objectives. For FRAP, a rectangular region with a width of approximately 215 nm, half of the hair bundle, or the whole hair bundle was photobleached for 1.1 – 1.6 s using 100% of the laser power from a 488 nm laser. In the section of the targeted bundle, even bleaching was confirmed by measuring the pixel intensity in the targeted region (Leica Application Suite Advanced Fluorescence (LAS AF) software; Leica Microsystems Inc.). Images were collected using 488 nm or 568 nm wavelengths. In some cases, the dynamic ranges of pixel intensities were modified for displaying samples with lower fluorescence signals; these modifications were not performed on images used for FRAP measurements. No saturated images were used in FRAP studies. For quantitative FRAP, single images were acquired (Snapp et al., 2003). For qualitative FRAP, multiple confocal images were averaged to decrease background fluorescence (Snapp et al., 2003).

For FRAP analyses, images were acquired and analyzed using imaging software (LAS AF; Leica Microsystems Inc.). To quantify the fluorescence recovery, the mean pixel value intensity of the bleached zone (region of interest 1, ROI 1), a non-bleached hair bundle (ROI 2) as a control, and a region that did not have high levels of fluorescence (ROI 3) for the background measurements at each time point were obtained automatically for short interval imaging (seconds) or manually for hourly imaging. The intensity of ROI 1 was corrected by subtracting the averaged intensity of ROI 3 and then adjusted for fluorescence loss due to photobleaching using ROI 2 in the same FRAP image series. For FRAP of fascin 2b fusion proteins and myosin XVa fusion protein, the following processing regime was used (Lippincott-Schwartz et al., 1999). Briefly, intensity in ROI 1 at each time point ($I(t)$) was subtracted by the corresponding ROI 3 intensity ($I_{background}$), $I_{b(t)} = I(t) - I_{background}$. The corrected intensity of ROI 1 at each time point ($I_b(t)$) was multiplied by a correction data set ($I_{precell}/I_{infcell}$) for photobleaching, $I_{b,corr}(t) = Ib(t)(I_{precell}/I_{infcell})$, where $I_{precell}$ represents the prebleached intensity of ROI 2 and $I_{infcel}\ l$ stands for post-bleached ROI 2 at the equilibrium time point—when the intensity of ROI 1 reached the plateau value. The equation, $I_{b,corr,normAxelrod}(t) = (I_{b,corr}(t) - Ib,corr(0))/(I_{b,corr}(inf) - Ib,corr(0))$, was used for normalization to rescale so that the plateau value is set to 100%, where $I_{b,corr}(t)$ is the intensity of ROI 1 at a given time point, $I_{b,corr}(0)$ is the intensity of ROI 1 immediately after the photobleaching time point, and $I_{b,corr}(inf)$ is the intensity at equilibrium (Axelrod et al., 1976). The recovery halftimes were determined from a normalized plot. To determine recovery half times, the data points were fit to a one-phase exponential equation (GraphPad Prism), $Y = Y0 + (plateau - Y0)(1- exp(-Kx))$, where $Y0$ is the Y value when x (time) is zero, *plateau* is the Y value at infinity, and K is the rate constant. Recovery half times ($t_{1/2}$) were calculated as $ln(2)/K$.

The percentage of total fluorescence recovery of β-actin-mCherry-containing hair bundles and GFP-fascin 2b-containing hair bundles was calculated using the equation, $100((I_{b,corr}(inf) - I_{b,corr}(0))/(I_{b,corr}(pre) - I_{b,corr}(0))$ (Feder et al., 1996; Snapp et al., 2003). Statistical analyses included Student's *t* tests (GraphPad, Prism). Recovery halftimes ($t_{1/2}$) are given as mean ± standard error of the mean (SEM).

Supplementary Material

Refer to Web version on PubMed Central for supplementary material.

Acknowledgments

We are grateful to C. Fernando for zebrafish husbandry, T. Friedman for myosin XVa cDNA, and Nilay Gupta for artwork. We thank E. Snapp for advice on FRAP studies and K. N. Alagramam, R. Stepanyan and members of our laboratory who provided discussion and comments on this manuscript. This research was supported by National Institutes of Health (NIH) Grants DC009437 (B.M.M.) and the Center for Clinical Research and Technology at University Hospitals Case Medical Center (B.M.M.). The NIH Office of Research Infrastructure Program (ORIP) award S10RR017980 supported research reported herein.

References

Anderson DW, Probst FJ, Belyantseva IA, Fridell RA, Beyer L, Martin DM, Wu D, Kachar B, Friedman TB, Raphael Y, et al. The motor and tail regions of myosin XV are critical for normal structure and function of auditory and vestibular hair cells. Hum Mol Genet. 2000; 9:1729–1738. [PubMed: 10915760]

Antonellis PJ, Pollock LM, Chou SW, Hassan A, Geng R, Chen X, Fuchs E, Alagramam KN, Auer M, McDermott BM Jr. ACF7is a hair-bundle antecedent, positioned to integrate cuticular plate actin and somatic tubulin. J Neurosci. 2014; 34:305–312. [PubMed: 24381291]

Aratyn YS, Schaus TE, Taylor EW, Borisy GG. Intrinsic dynamic behavior of fascin in filopodia. Mol Biol Cell. 2007; 18:3928–3940. [PubMed: 17671164]

Axelrod D, Koppel DE, Schlessinger J, Elson E, Webb WW. Mobility measurement by analysis of fluorescence photobleaching recovery kinetics. Biophys J. 1976; 16:1055–1069. [PubMed: 786399]

Balciunas D, Wangensteen KJ, Wilber A, Bell J, Geurts A, Sivasubbu S, Wang X, Hackett PB, Largaespada DA, McIvor RS, et al. Harnessing a high cargo-capacity transposon for genetic applications in vertebrates. PLoS Genet. 2006; 2:e169. [PubMed: 17096595]

Bartles JR. Parallel actin bundles and their multiple actin-bundling proteins. Curr Opin Cell Biol. 2000; 12:72–78. [PubMed: 10679353]

Belyantseva IA, Boger ET, Friedman TB. Myosin XVa localizes to the tips of inner ear sensory cell stereocilia and is essential for staircase formation of the hair bundle. Proc Natl Acad Sci USA. 2003; 100:13958–13963. [PubMed: 14610277]

Belyantseva IA, Boger ET, Naz S, Frolenkov GI, Sellers JR, Ahmed ZM, Griffith AJ, Friedman TB. Myosin-XVa is required for tip localization of whirlin and differential elongation of hair-cell stereocilia. Nat Cell Biol. 2005; 7:148–156. [PubMed: 15654330]

Belyantseva IA, Perrin BJ, Sonnemann KJ, Zhu M, Stepanyan R, McGee J, Frolenkov GI, Walsh EJ, Friderici KH, Friedman TB, et al. Gamma-actin is required for cytoskeletal maintenance but not development. Proc Natl Acad Sci USA. 2009; 106:9703–9708. [PubMed: 19497859]

Boeda B, El-Amraoui A, Bahloul A, Goodyear R, Daviet L, Blanchard S, Perfettini I, Fath KR, Shorte S, Reiners J, et al. Myosin VIIa, harmonin and cadherin 23, three Usher I gene products that cooperate to shape the sensory hair cell bundle. EMBO J. 2002; 21:6689–6699. [PubMed: 12485990]

Chou SW, Hwang PS, Gomez G, Fernando CA, West MC, Pollock LM, Lin-Jones J, Burnside B, McDermott BM. Fascin 2b is a component of stereocilia that lengthens actin-based protrusions. PLoS ONE. 2011; 6:e14807. [PubMed: 21625653]

Courson DS, Rock RS. Actin cross-link assembly and disassembly mechanics for alpha-Actinin and fascin. J Biol Chem. 2010; 285:26350–26357. [PubMed: 20551315]

Daudet N, Lebart MC. Transient expression of the t-isoform of plastins/fimbrin in the stereocilia of developing auditory hair cells. Cell Motil Cytoskeleton. 2002; 53:326–336. [PubMed: 12378542]

Drummond MC, Barzik M, Bird JE, Zhang DS, Lechene CP, Corey DP, Cunningham LL, Friedman TB. Live-cell imaging of actin dynamics reveals mechanisms of stereocilia length regulation in the inner ear. Nat Commun. 2015; 6:6873. [PubMed: 25898120]

Edds KT. Dynamic aspects of filopodial formation by reorganization of microfilaments. J Cell Biol. 1977; 73:479–491. [PubMed: 558198]

Feder TJ, Brust-Mascher I, Slattery JP, Baird B, Webb WW. Constrained diffusion or immobile fraction on cell surfaces: a new interpretation. Biophys J. 1996; 70:2767–2773. [PubMed: 8744314]

Friedman TB, Hinnant JT, Fridell RA, Wilcox ER, Raphael Y, Camper SA. DFNB3 families and Shaker-2 mice: mutations in an unconventional myosin, myo 15. Adv Otorhinolaryngol. 2000; 56:131–144. [PubMed: 10868225]

Gibson F, Walsh J, Mburu P, Varela A, Brown KA, Antonio M, Beisel KW, Steel KP, Brown SD. A type VII myosin encoded by the mouse deafness gene shaker-1. Nature. 1995; 374:62–64. [PubMed: 7870172]

Gorelik J, Shevchuk AI, Frolenkov GI, Diakonov IA, Lab MJ, Kros CJ, Richardson GP, Vodyanoy I, Edwards CR, Klenerman D, et al. Dynamic assembly of surface structures in living cells. Proc Natl Acad Sci USA. 2003; 100:5819–5822. [PubMed: 12721367]

Jia S, Yang S, Guo W, He DZ. Fate of mammalian cochlear hair cells and stereocilia after loss of the stereocilia. J Neurosci. 2009; 29:15277–15285. [PubMed: 19955380]

Kee HL, Dishinger JF, Blasius TL, Liu CJ, Margolis B, Verhey KJ. A size-exclusion permeability barrier and nucleoporins characterize a ciliary pore complex that regulates transport into cilia. Nat Cell Biol. 2012; 14:431–437. [PubMed: 22388888]

Kimmel CB, Patterson J, Kimmel RO. The development and behavioral characteristics of the startle response in the zebra fish. Dev Psychobiol. 1974; 7:47–60. [PubMed: 4812270]

Li A, Dawson JC, Forero-Vargas M, Spence HJ, Yu X, Konig I, Anderson K, Machesky LM. The actin-bundling protein fascin stabilizes actin in invadopodia and potentiates protrusive invasion. Curr Biol. 2010; 20:339–345. [PubMed: 20137952]

Lin-Jones J, Burnside B. Retina-specific protein fascin 2 is an actin cross-linker associated with actin bundles in photoreceptor inner segments and calycal processes. Invest Ophthalmol Vis Sci. 2007; 48:1380–1388. [PubMed: 17325187]

Lippincott-Schwartz J, Presley JF, Zaal KJ, Hirschberg K, Miller CD, Ellenberg J. Monitoring the dynamics and mobility of membrane proteins tagged with green fluorescent protein. Methods Cell Biol. 1999; 58:261–281. [PubMed: 9891386]

Manley GA. Evolutionary paths to mammalian cochleae. J Assoc Res Otolaryngol. 2012; 13:733–743. [PubMed: 22983571]

Manor U, Kachar B. Dynamic length regulation of sensory stereocilia. Semin Cell Dev Biol. 2008; 19:502–510. [PubMed: 18692583]

McDermott BM Jr, Asai Y, Baucom JM, Jani SD, Castellanos Y, Gomez G, McClintock JM, Starr CJ, Hudspeth AJ. Transgenic labeling of hair cells in the zebrafish acousticolateralis system. Gene Expr Patterns. 2010; 10:113–118. [PubMed: 20085825]

Narayanan P, Chatterton P, Ikeda A, Ikeda S, Corey DP, Ervasti JM, Perrin BJ. Length regulation of mechanosensitive stereocilia depends on very slow actin dynamics and filament-severing proteins. Nat Commun. 2015; 6:6855. [PubMed: 25897778]

Perrin BJ, Strandjord DM, Narayanan P, Henderson DM, Johnson KR, Ervasti JM. Beta-actin and fascin-2 cooperate to maintain stereocilia length. J Neurosci. 2013; 33:8114–8121. [PubMed: 23658152]

Rzadzinska AK, Schneider ME, Davies C, Riordan GP, Kachar B. An actin molecular treadmill and myosins maintain stereocilia functional architecture and self-renewal. J Cell Biol. 2004; 164:887–897. [PubMed: 15024034]

Schwander M, Kachar B, Muller U. Review series: The cell biology of hearing. J Cell Biol. 2010; 190:9–20. [PubMed: 20624897]

Shin JB, Krey JF, Hassan A, Metlagel Z, Tauscher AN, Pagana JM, Sherman NE, Jeffery ED, Spinelli KJ, Zhao H, et al. Molecular architecture of the chick vestibular hair bundle. Nat Neurosci. 2013; 16:365–374. [PubMed: 23334578]

Shin JB, Longo-Guess CM, Gagnon LH, Saylor KW, Dumont RA, Spinelli KJ, Pagana JM, Wilmarth PA, David LL, Gillespie PG, et al. The R109H variant of fascin-2, a developmentally regulated

actin crosslinker in hair-cell stereocilia, underlies early-onset hearing loss of DBA/2J mice. J Neurosci. 2010; 30:9683–9694. [PubMed: 20660251]

Snapp EL, Altan N, Lippincott-Schwartz J. Measuring protein mobility by photobleaching GFP chimeras in living cells. Curr Protoc Cell Biol. 2003 *Ch. 21*, Unit 21.1.

Svitkina TM, Bulanova EA, Chaga OY, Vignjevic DM, Kojima S, Vasiliev JM, Borisy GG. Mechanism of filopodia initiation by reorganization of a dendritic network. J Cell Biol. 2003; 160:409–421. [PubMed: 12566431]

Tilney LG, Derosier DJ, Mulroy MJ. The organization of actin filaments in the stereocilia of cochlear hair cells. J Cell Biol. 1980; 86:244–259. [PubMed: 6893452]

Vignjevic D, Kojima S, Aratyn Y, Danciu O, Svitkina T, Borisy GG. Role of fascin in filopodial protrusion. J Cell Biol. 2006; 174:863–875. [PubMed: 16966425]

Vollrath MA, Kwan KY, Corey DP. The micromachinery of mechanotransduction in hair cells. Annu Rev Neurosci. 2007; 30:339–365. [PubMed: 17428178]

Zhang DS, Piazza V, Perrin BJ, Rzadzinska AK, Poczatek JC, Wang M, Prosser HM, Ervasti JM, Corey DP, Lechene CP. Multi-isotope imaging spectrometry reveals protein turnover in hair-cell stereocilia. Nature. 2012; 481:520–524. [PubMed: 22246323]

Zhao Y, Yamoah EN, Gillespie PG. Regeneration of broken tip links and restoration of mechanical transduction in hair cells. Proc Natl Acad Sci USA. 1996; 93:15469–15474. [PubMed: 8986835]

Zheng L, Sekerkova G, Vranich K, Tilney LG, Mugnaini E, Bartles JR. The deaf jerker mouse has a mutation in the gene encoding the espin actin-bundling proteins of hair cell stereocilia and lacks espins. Cell. 2000; 102:377–385. [PubMed: 10975527]

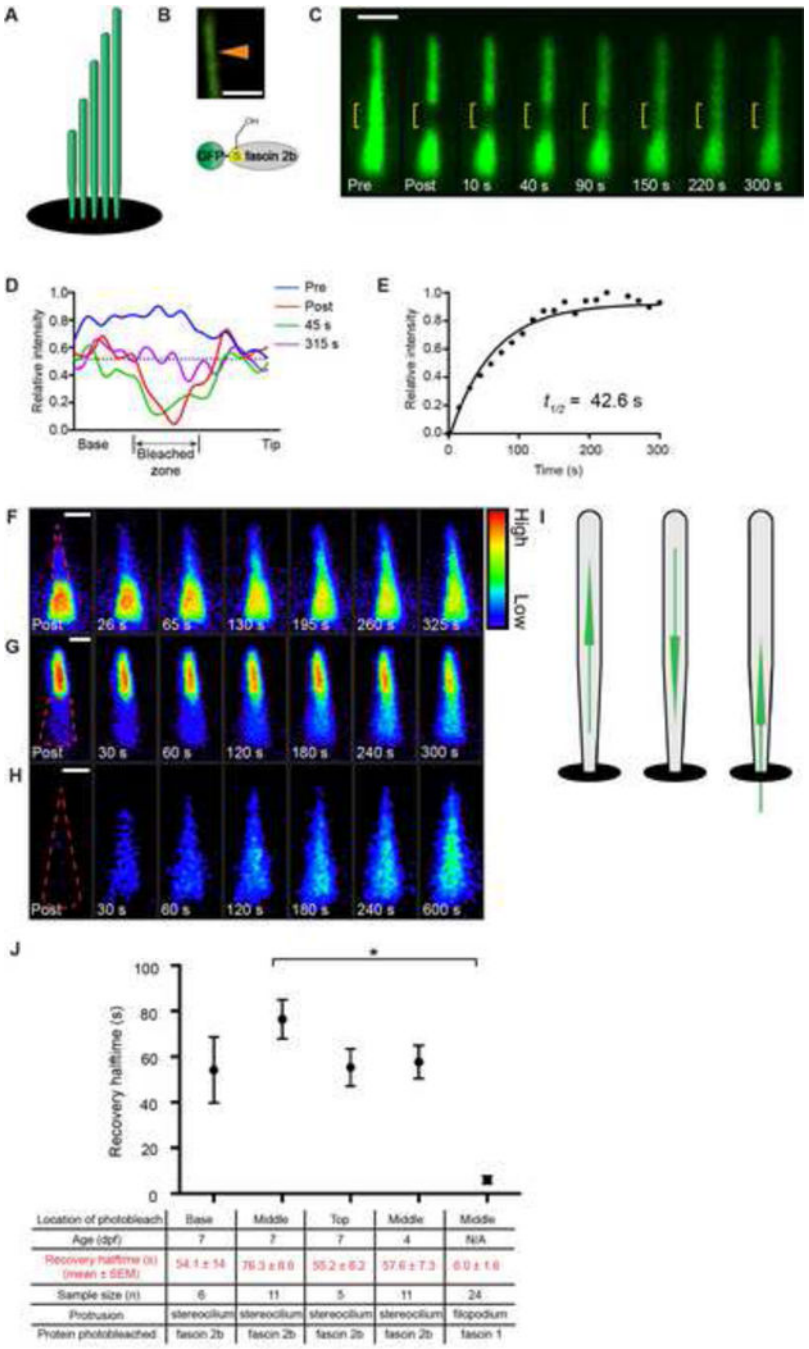

Figure 1. Stereociliary fascin 2b exchanges rapidly and without bias

(**A**) Hair bundle schematic (**B**) (top) Confocal image of a single stereocilium (arrowhead) containing GFP-fascin 2b (green) demonstrates even labeling of the protrusion's core. Below is a schematic of the fusion protein. (**C**) A lateral crista hair bundle before (Pre) and after a photobleach, which targeted the mid-region (yellow bracket). This FRAP series is qualitative. (**D**) FRAP profiles from a quantitative series of images displayed in Figure S1A. Within 315 s, the mean intensity in the post-bleached region nearly matches the mean intensity along the length of the stereocilia (dashed line), indicating significant GFP-fascin

2b exchange. (**E**) Recovery plot from quantitative FRAP series in Figure S1A fit to a one-phase exponential function. Color-coded scale of recovery, after upper half (**F**) or lower half (**G**) of bundles were bleached (dashed line), demonstrates that GFP-fascin 2b migrates towards the stereociliary tips or bases, respectively. Blue-to-red color scale represents low-to-high GFP signal, respectively. (**H**) Bleaching entire bundle reveals migration of fusion protein from soma to stereocilia. (**I**) Models of fascin 2b movement in stereocilia. (**J**) Mean FRAP recovery halftimes from photobleach events of tops, middles, or bases of hair bundles containing GFP-fascin 2b from 7- or 4-dpf zebrafish or from middles of filopodia containing GFP-fascin 1 from COS-7 cells (Aratyn et al., 2007). *$P < 0.005$ (Student's *t* test) indicates statistically distinct. Scale bars are 1 μm. See also Figures S1, S2, and S4, Tables S1 and S2, and Movie S1.

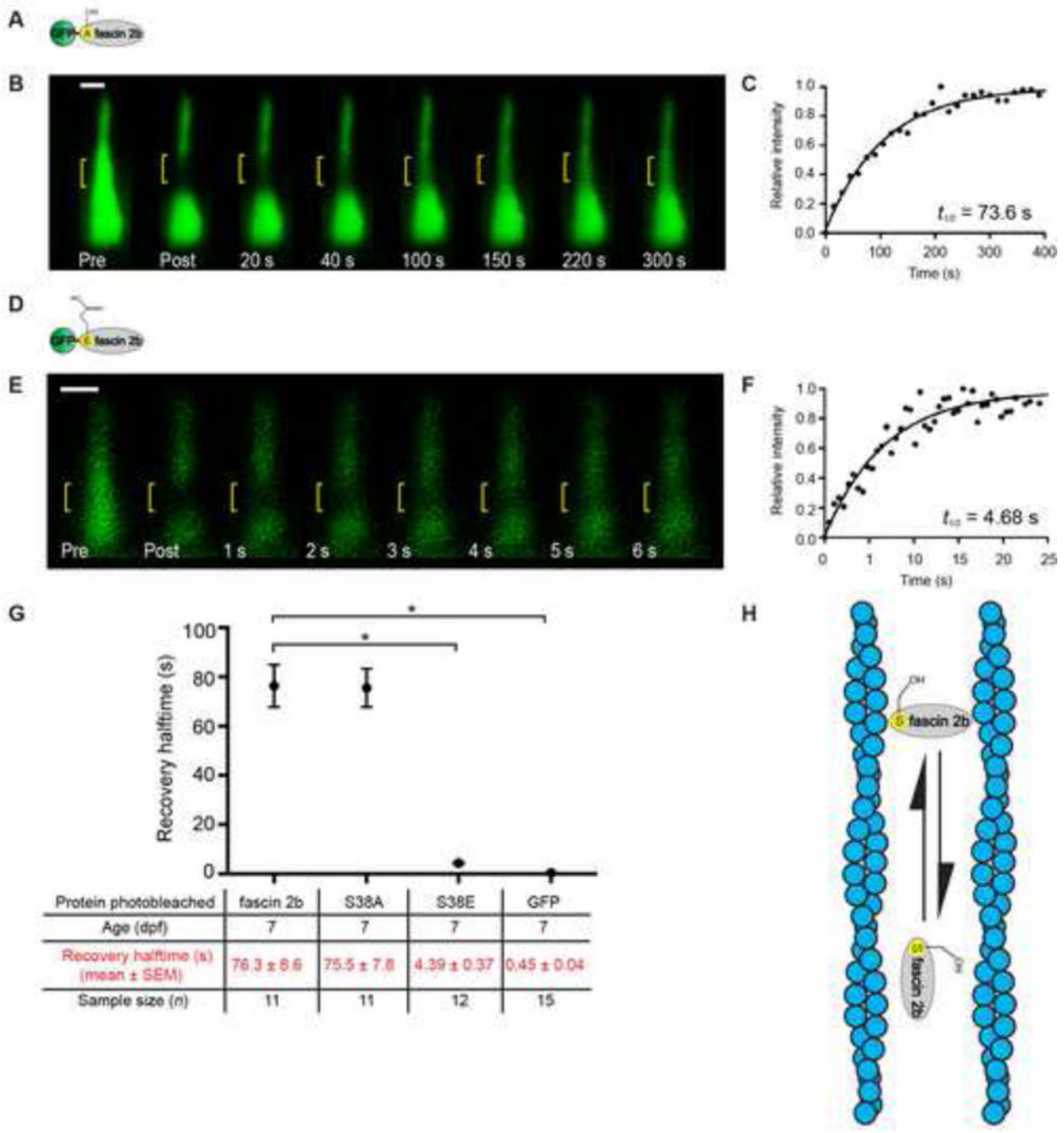

Protein photobleached	fascin 2b	S38A	S38E	GFP
Age (dpf)	7	7	7	7
Recovery halftime (s) (mean ± SEM)	76.3 ± 8.6	75.5 ± 7.8	4.39 ± 0.37	0.45 ± 0.04
Sample size (*n*)	11	11	12	15

Figure 2. Rapid stereociliary fascin 2b exchange transpires without a phosphointermediate

(**A**) Phosphomutant GFP-S38A fascin 2b schematic. (**B**) Qualitative FRAP series of a hair bundle containing GFP-S38A fascin 2b before (Pre) and after photobleaching (yellow bracket). (C) Recovery plot from a hair bundle containing GFP-S38A fascin 2b from a quantitative FRAP series in Figure S1F, $t_{1/2}$ = 73.6 s. (**D**) Phosphomimetic GFP-S38E fascin 2b schematic. (**E**) Bundle containing GFP-S38E fascin 2b before (Pre) and after photobleaching. (**F**) Recovery plot of **E** demonstrates exceedingly fast recovery, $t_{1/2}$ = 4.68 s, of the phosphomimetic relative to wild-type fascin 2b. (**G**) Summary of recovery

halftimes for GFP-fascin 2b, GFP-S38A fascin 2b (S38A), GFP-S38E fascin 2b (S38E), and GFP. Since GFP-S38A fascin 2b has a similar $t_{1/2}$ value to GFP-fascin 2b, wild-type fascin 2b does not transition through a detectable phosphointermediate in stereocilia. *P< 0.0001 (Student's t test) indicates statistically significant. Fish used were 7 dpf. Scale bars are 1 μm. (**H**) Model: The fascin 2b-F-actin binding cycle is independent of phosphorylation. In model, horizontally oriented fascin 2b protein indicates protein bound to F-actin. Vertically oriented fascin 2b protein is not bound to F-actin. Alternative model is shown in Figure S3B. See also Figure S3 and Tables S1 and S3.

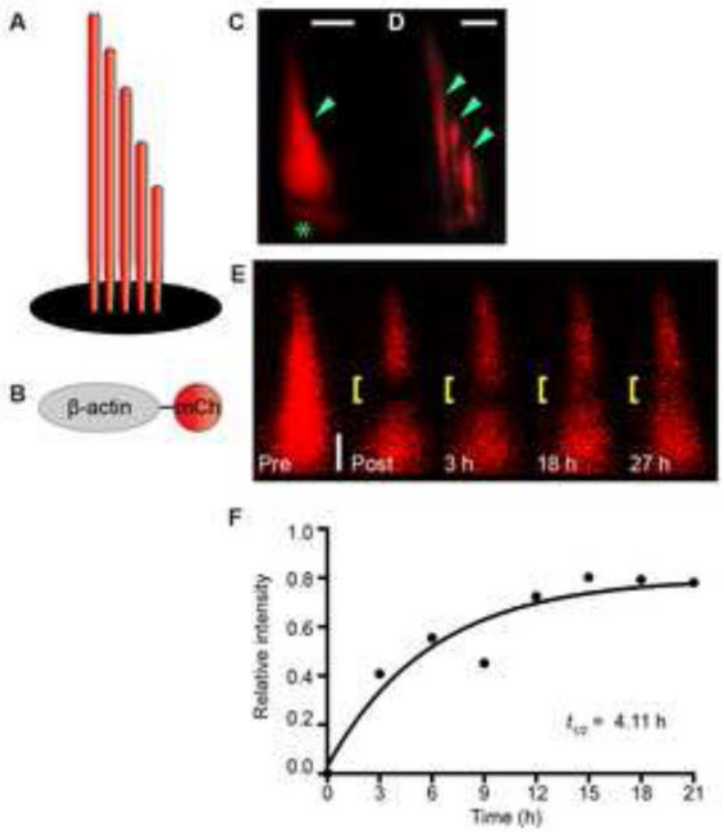

Figure 3. β-actin exchanges on an hourly timescale in live zebrafish hair cells

Schematics of a hair bundle (**A**) and β-actin-mCherry (**B**). (**C**) Hair bundle (arrowhead) and cuticular plate (asterisk) labeled with *β*-actin-mCherry in transgenic zebrafish. (**D**) Confocal image of three stereocilia (arrowheads) from a splayed hair bundle reveals even labeling across each stereocilium. Splayed bundles are rare in this transgenic. Note: limited portions of each stereocilium are in the plane of focus. (**E**) Quantitative fluorescence recovery of a bundle containing β-actin-mCherry after a midsection bleach (yellow bracket). (**F**) Recovery plot reveals a $t_{1/2}$ of 4.11 h for the hair bundle observed in **E**. The data points are fit to a one-phase exponential equation. Zebrafish examined at 7 dpf. Scale bar is 1 μm. See also Figure S4 and Table S1.

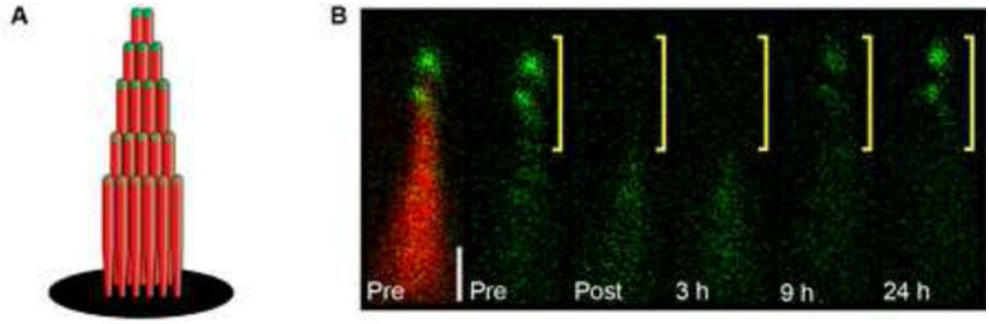

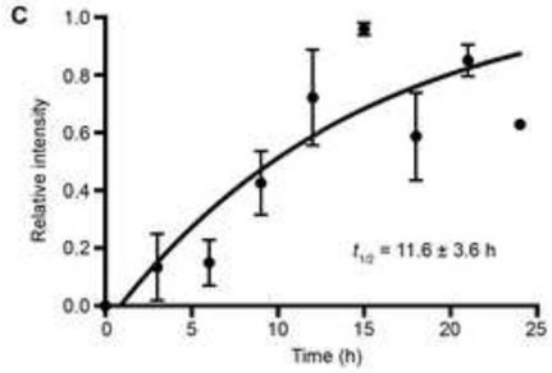

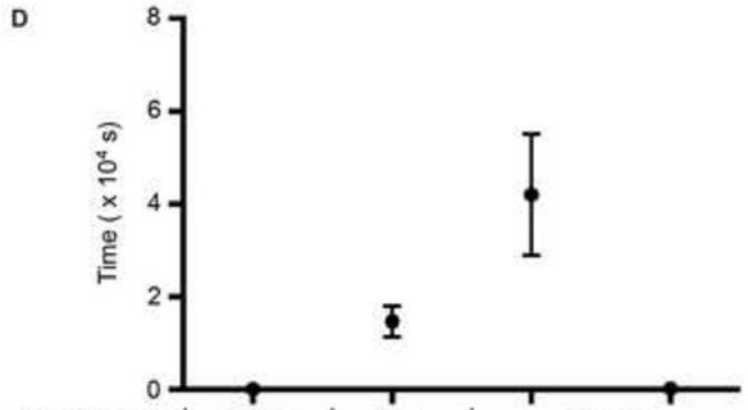

Protein photobleached	fascin 2b	β-actin	Myosin XVa	
Protrusion	stereocilia	stereocilia	stereocilia	filopodia
Recovery halftime (s) (mean ± SEM)	76.3 ± 8.6	(1.46 ± 0.32) x 10^4	(4.20 ± 1.3) x 10^4	2.4 x 10^4
Sample size (*n*)	11	10	4	2

Figure 4. Robust myosin XVa exchange at the tips of mature stereocilia

(**A**) Schematic of bundle containing β-actin-mCherry (red) and GFP-myosin XVa (green). (**B**) Image of a bundle expressing GFP-myosin XVa (green) reveals fusion protein at stereociliary tips (Pre, left and right). Bundle is counterlabeled with β-actin-mCherry (Pre, left, red) in a doubly transgenic hair cell. After photobleaching the top half of bundle (only GFP signal is shown), the GFP-myosin XVa signal recovers completely by 24 h. Scale bar is 1 μm. (**C**) Time course of myosin XVa recovery. Zebrafish examined at 7 dpf. (**D**) Summary

of recovery halftimes of fusion proteins in stereocilia and filopodia. Recovery halftime of myosin XVa in filopodia is estimated (Belyantseva et al., 2005). See also Table S1.